IMPROVING PROTOCOLS

Dual-source computed tomography protocols for the pediatric chest — scan optimization techniques

Jordan B. Rapp[1,2] · Victor M. Ho-Fung[1,2] · Karen I. Ramirez[1] · Ammie M. White[1,2] · Hansel J. Otero[1,2] · David M. Biko[1,2]

Abstract

The gold standard for pediatric chest imaging remains the CT scan. An ideal pediatric chest CT has the lowest radiation dose with the least motion degradation possible in a diagnostic scan. Because of the known inherent risks and costs of anesthesia, non-sedate options are preferred. Dual-source CTs are currently the fastest, lowest-dose CT scanners available, utilizing an ultra-high-pitch mode resulting in sub-second CTs. The dual-energy technique, available on dual-source CT scanners, gathers additional information such as pulmonary blood volume and includes relative contrast enhancement and metallic artifact reduction, features that are not available in high-pitch flash mode. In this article we discuss the benefits and tradeoffs of dual-source CT scan modes and tips on image optimization.

Keywords Chest · Children · Computed tomography · Dual energy · Dual source · Metal reduction · Ultra-high pitch

Introduction

Despite advances in MRI, CT remains the gold standard for imaging the pediatric chest, particularly when it comes to imaging the lung parenchyma. Single-source CT was the mainstay of CT imaging for the modality's first 30 years. In 2006, the first dual-source system was introduced by Siemens Healthineers (Forchheim, Germany). This system had two energy sources and two associated detectors, allowing two energy sources to be applied at different energy levels simultaneously: dual-energy CT. Alternatively, both energy sources could be used at the same energy level simultaneously with an ultra-high pitch, allowing for faster scans and greater temporal resolution. Here we discuss how these scan parameters can be used and best applied to pediatric chest imaging. Alternative approaches for dual-energy CT (e.g., split beam, dual-layer detector, split filter, etc.) are beyond the scope of this review [1].

✉ Jordan B. Rapp
  rappj@chop.edu

1 Department of Radiology, Children's Hospital
   of Philadelphia, 3401 Civic Center Blvd., Philadelphia,
   PA 19104, USA

2 Perelman School of Medicine, University of Pennsylvania,
   Philadelphia, PA, USA

Three generations of scanners

The initial dual-source scanner was released by Siemens in 2006 and featured a very similar setup to today's third-generation scanner. In all iterations, both X-ray sources have been located orthogonally; they were 90° apart in the first generation, and 95° apart in subsequent generations (Fig. 1). The lower-energy tube has a minimum 80 kVp in the first and second generations in dual-energy mode, while in the third generation this was brought down to 70 kVp. Meanwhile, the higher-energy tube maximum kilovoltage peak was initially set at 140 kVp and later at 150 kVp on the third generation. A tin filter was added to the high-energy tube on second- and third-generation scanners to filter out the low-energy beams and improve spectral separation and dose efficiency [2]. The field of view (FOV) is smaller in the high-energy tube, increased in subsequent generations up to 35.5 cm, while the low-energy FOV has remained larger at 50 cm. This smaller FOV can limit evaluation of tissues that fall outside of it, which can be an issue with larger patients and most often only involves the soft tissue of the chest wall [3]. Each iteration has also resulted in improved scan speeds, with a gantry speed now as fast as 0.25 s resulting in a temporal resolution of 66 ms. The three generations of scanners are outlined in Table 1.

Fig. 1 Diagram depicts the third-generation dual-source scanner. Two tubes are located 95° apart. The lower-kilovoltage (kV) tube (*blue*) has a larger field of view (50 cm), while the higher-kV tube (*orange*) has a smaller field of view (35 cm)
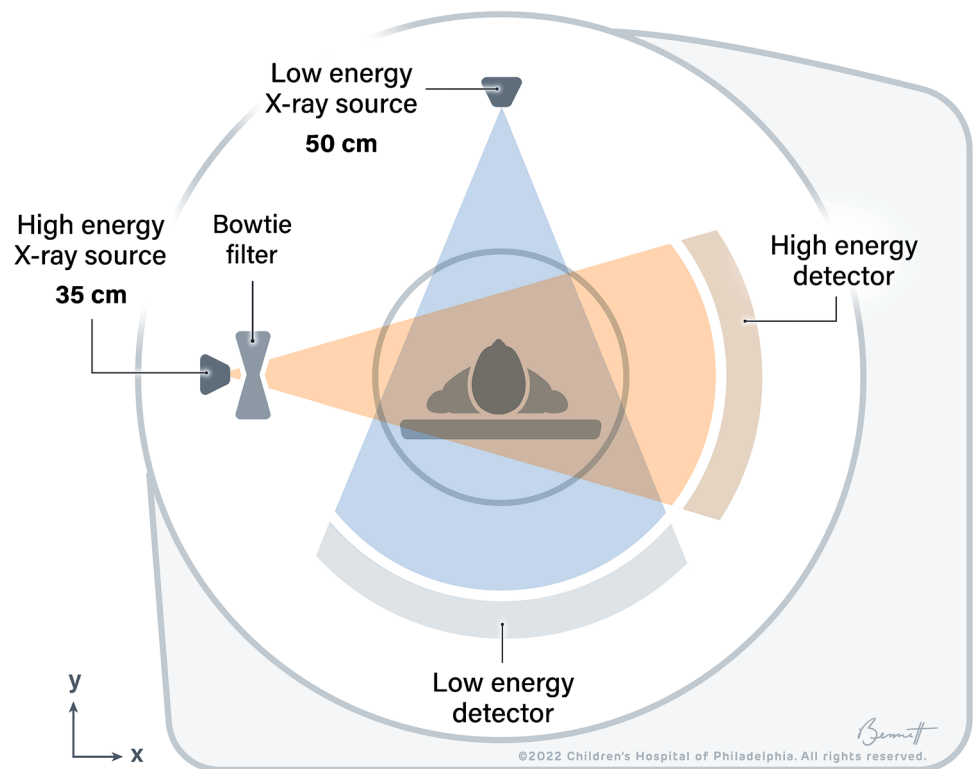

Table 1 Three generations of dual-source CT scanners

Features	1st generation[a] (2006)	2nd generation[b] (2009)	3rd generation[c] (2014)
Low/high kVp	80/140	80/140 Sn	70/150 Sn (80/150 Sn)[d]
High−/low-detector FOV (cm)	26/50	33/50	35.5/50
Tube separation (°)	90	95	95
Gantry speed (s)	0.33	0.28	0.25
Detector slices (n)	64	128	196
Slice thickness (mm)	0.6	0.6	0.6

cm centimeters, *FOV* field of view, *kVp* kilovoltage peak, *mm* millimeters, *n* number, *s* seconds, *Sn* tin filter added

[a] 1st generation: Siemens Definition

[b] 2nd generation: Siemens Definition FLASH

[c] 3rd generation: Siemens FORCE

[d] High/low kVp range settings for chest imaging, for the third generation the narrower range of 80/150 Sn is ideal for larger patients, while the 70/150 Sn is designed for smaller patients

Sedation

The improved temporal resolution of dual-source CT is extremely beneficial for reducing the need for sedation in the younger pediatric population, or in any population prone to movement such as the uncooperative child. Faster scans result in less motion artifact in non-sedated children. In pediatric patients younger than 4–6 months, scanning can be attempted using a feed-and-swaddle technique to avoid sedation, regardless of scanner type. However, children who are too young to follow directions but too old to respond to feed-and-swaddle often require some sedation to allow for a motion-minimized or motion-free study.

While general anesthesia with a breath-hold is the only way to guarantee a motion-free study, it does not come without limitations. General anesthesia is known to result in some atelectasis, usually in the dependent lungs, which can obscure lung nodules/masses or confound interpretation of infection or aspiration [4, 5]. Perhaps just as important is a possible association between multiple general anesthesia events with neurotoxicity and brain development, particularly in the young growing brain, the same population that

is most likely to have their scans improved with anesthesia [6–8]. Children can also sustain minor short-term adverse events of sedation and anesthesia such as nausea and vomiting [9]. More severe adverse events such as cardiac arrest or neurologic injury, while rare, more commonly occur in children with one or more comorbidities [10]. Additionally, sedation and anesthesia increase the cost and time to perform a study and can strain resources. Therefore, it is advisable to avoid sedation or general anesthesia when possible.

Using a second-generation dual-source scanner, Kino et al. [11] compared the performance of chest CT with general anesthesia using breath-holds to the performance of free-breathing scans. In their cohort of 86 children ages 3 and younger, the authors concluded that while image quality was improved with general anesthesia, quality remained sufficient for diagnosis without anesthesia using the high-pitch scans [11]. Similarly, Tivnan et al. [12] assessed image quality in children younger than 6 years undergoing CT angiography on a third-generation dual-source CT scanner with and without general anesthesia. In their cohort of 73 children, they similarly found that while motion artifact was greater without anesthesia, only a small minority of non-anesthesia cases were non-diagnostic [12].

Electrocardiography-gated synchronization

To enhance cardiac and vascular scanning, electrocardiography (ECG)-gated synchronization is often required to obtain diagnostic imaging. Three primary modes of ECG-gated synchronization can be used on a dual-source scanner: ECG gating with ultra-high pitch, prospective ECG gating and retrospective ECG gating. ECG gating with ultra-high pitch enables scanning of the heart during a single heartbeat by timing the table position and acceleration with the child's heart position and selected phase of the cardiac cycle [13]. This results in an image of the heart without cardiac motion. In prospective ECG gating, the child is scanned sequentially during the same point in the cardiac cycle over multiple heartbeats to reconstruct a motion-free image. Retrospectively ECG-gated studies involve imaging over the entire cardiac cycle. This technique can be used to measure cardiac function and is also helpful in the presence of a cardiac arrhythmia or for visualization of the coronary arteries, which is beyond the scope of this review [14, 15]. When ECG gating is being used, it is not possible to perform a dual-energy CT at the same time.

Scanner modes

Standard pitch

The single-source mode is considered the standard mode. This is when neither high-pitch nor dual-energy mode is being used. A table pitch of up to 1.5 (range 0.5–1.5) is used for standard mode. While standard mode suffices for most types of imaging with cooperative patients, it lacks the benefits of ultra-high-pitch and dual-energy modes, detailed in the next sections. Standard pitch mode is not ideal for situations where there is motion, such as when evaluating large vessels and the heart [16].

Standard pitch mode on the dual-source system can be performed as low as 70 kV on second- and third-generation scanners. This setting is ideal for lowering radiation dose in the youngest of children and also results in improved contrast conspicuity because it is nearer to the k-edge of iodine.

Dynamic airway imaging also uses both energy tubes at the same energy for a rapid scan, though without table movement, using axial scan mode with greater temporal resolution than can be offered on single-source scanners [16]. This allows the child's airway to be scanned multiple times per respiratory cycle during free-breathing in awake children, and has compared favorably to bronchoscopy (Fig. 2) [17]. It can also be used to titrate the child's peak end-expiratory pressure requirements [18].

Ultra-high pitch

The high-pitch mode's greatest benefits are in the non-sedate child who is prone to motion artifact. Additionally, this mode is often used with angiographic studies. This technique is only available on dual-source scanners that can reach a pitch of greater than 3. Because the two energy beams are offset by 90–95°, dual-source scanners can effectively double the pitch, reaching a maximum pitch of 3.4 with minimal noticeable sampling artifact. This high-pitch mode has been shown to lessen respiratory artifact while simultaneously decreasing radiation dose in pediatric chest imaging [19, 20]. As with standard mode, ultra-high-pitch mode can be performed as low as 70 kV.

Dual energy

The principles of material decomposition and image generation have been discussed elsewhere and are beyond the scope of this review [2]. It is important to note here that when dual-energy mode is employed, the ultra-high-pitch mode cannot be used. Dual-energy mode requires each tube to operate at different energy levels and therefore at a lower pitch. This loss of temporal resolution results in susceptibility to cardiac motion, vascular pulsation and respiratory motion. Angiographic studies, particularly when looking for precise measurements as in the aortic root, are less ideally performed with dual energy. However, dual energy offers additional information not otherwise available in standard or ultra-high-pitch modes.

Fig. 2 Dynamic airway CT in a 5-month-old girl with a history of tracheoesophageal fistula status post repair with continued need for ventilatory support. CT was performed with a second-generation scanner at 80 kVp and 6 mAs. Multiple images were obtained at the same level without table movement. **a, b** Axial CT in maximum collapse (**a**) and maximum distention (**b**) during free-breathing. **c, d** Coronal reconstruction images in maximum collapse (**c**) and maximum distension (**d**) demonstrate severe tracheal stenosis at site of the surgical repair. *L* left, *R* right
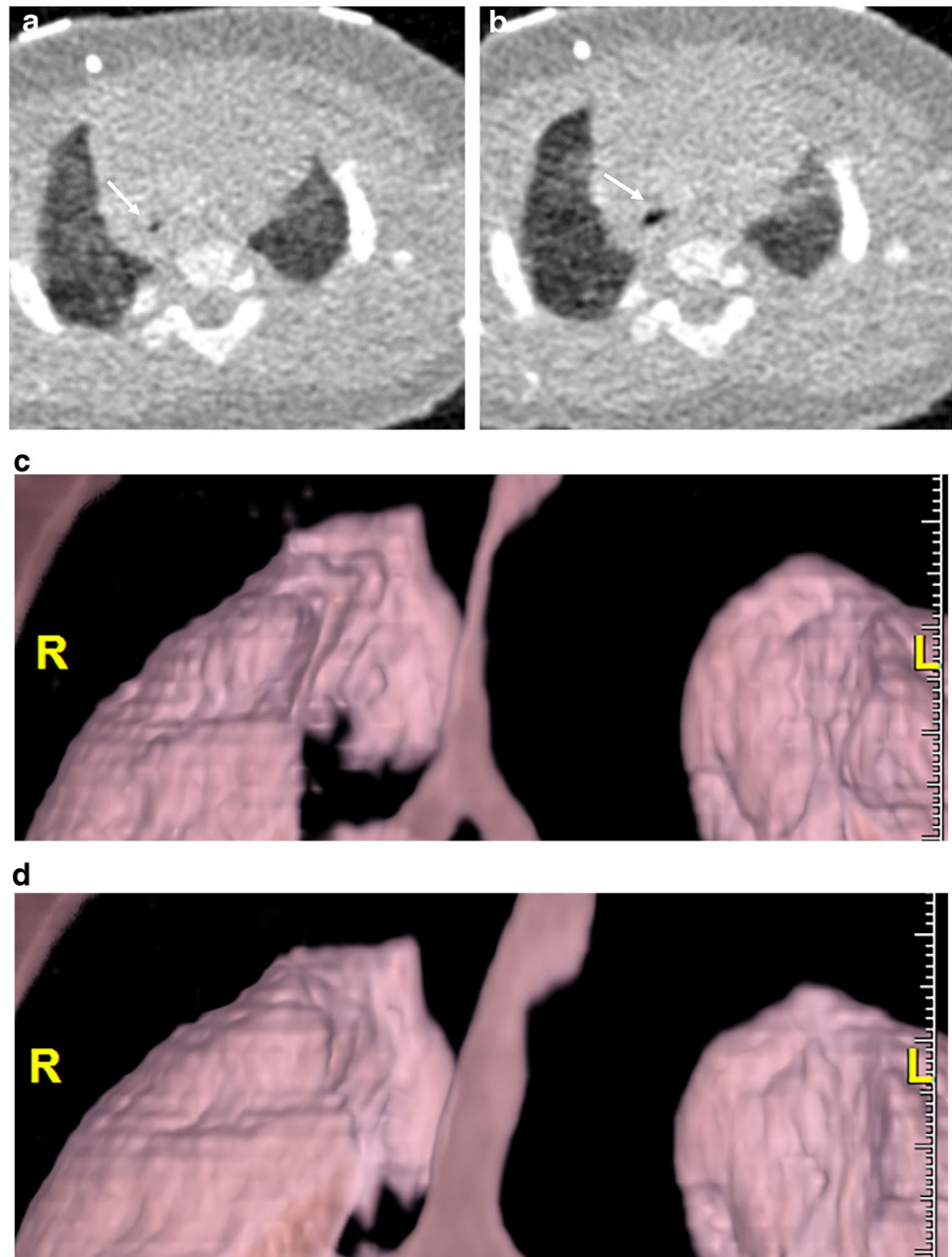
Available post-processing imaging output options in dual-energy chest imaging include virtual non-contrast, monoenergetic+, pulmonary blood volume and iodine maps. Virtual non-contrasts are paired with iodine maps. In these images, contrast is either subtracted from the image (virtual non-contrast) or overlayed on to the anatomical CT images (iodine map) (Fig. 3). This technique can help determine whether a lesion is truly enhancing. The iodine maps can also be used for quantifying the concentration of iodine in a lesion [21]. The virtual non-contrast image also lessens the need for a non-contrast phase of scanning, thereby reducing radiation dose.

Monoenergetic+ works by extrapolating the energies beyond the initial data sets, with an available range of 40 keV to 190 keV. Lower energies are closer to the k-edge of iodine, which is useful for improving visualization of contrast medium, potentially decreasing the amount of contrast medium that can be given, or rescuing a poor bolus [22, 23]. Conversely, high energies can help suppress metal artifact, discussed in greater detail later [24].

Pulmonary blood volume technique is useful for assessing lung perfusion. This technique is best applied when timing contrast administration to the right heart or pulmonary artery in order to best mimic blood flow to the lung. This is presented as
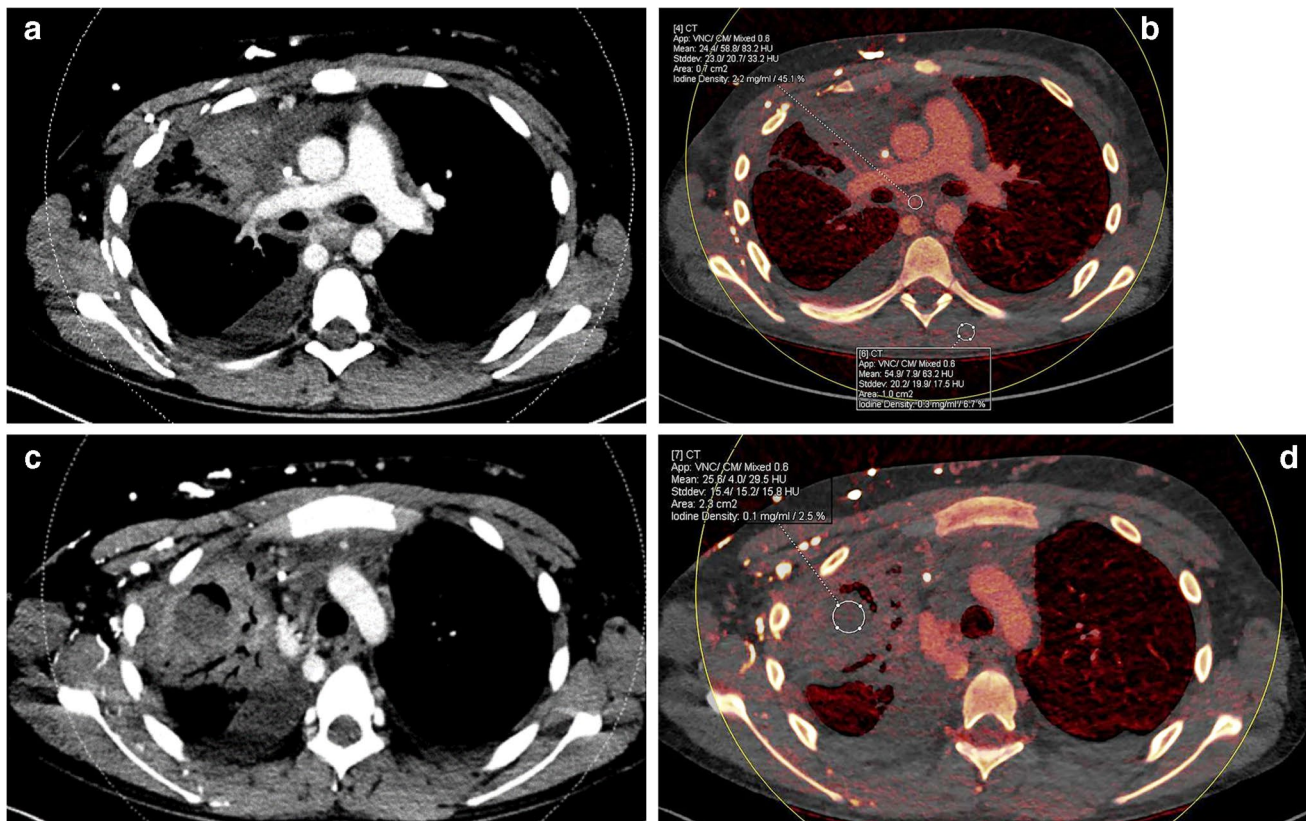
Fig. 3 Dual-energy techniques in a 15-year-old boy with a history of recurrent diffuse large B cell lymphoma. **a** Axial CT image through the chest in soft-tissue window demonstrates a subcarinal enhancing lymph node. **b** Axial CT iodine map overlay shows an iodine density of 2.2 mg/mL while the background musculature is 0.3 mg/mL. **c, d** Axial CT of the chest in soft-tissue window (**c**) shows a right-upper-lobe lung abscess, with axial iodine overlay (**d**) demonstrating no significant iodine uptake within the abscess

a color overlay, with perfusion defects present in areas of poor or diminished flow as represented by a lower scale color or absence of color [25] (Fig. 4). Importantly, atelectatic lung might appear as non-perfused, and therefore the anatomical images must be viewed in concert [26]. When imaging lung that is denser, such as in atelectasis or in intrinsically dense lungs such as in neonates, older infants and those with chronic lung disease, one should use the "dense lung" tool [27]. This change results in increased maximal Hounsfield units analyzed, ultimately including perfused lung that would otherwise be missed (Fig. 5).

Dual-energy post-processing protocols can be set up to be automatically performed. As an additional "reconstruction" job after a dual-energy CT is performed, the CT workstation can autotask the high- and low-kVp data series to be sent to a separate workstation with Syngo.via, Siemens' (Forchheim) proprietary post-processing software, installed. From there, the chosen algorithm is performed, be it pulmonary blood volume, monoenergetic+ (at a chosen level, i.e. 50 keV for iodine), iodine maps and virtual non-contrast. When this is completed, the series is automatically exported to be viewed and interpreted by the radiologist. When the radiologist needs additional information that is not provided by the automatic post-processing, the radiologist

can access the data within the application and manually post-process the images. Furthermore, the two data sets obtained at the high and low kVp are merged and produce a blended or mixed image, also available for interpretation immediately, which appears as single-energy images. Table 2 describes dual-energy imaging output options based on scan indication.

Protocols

Unenhanced computed tomography scan

Most unenhanced CT chest indications are to evaluate the lung parenchyma, such as for interstitial lung disease, certain tumors (e.g., metastasis from osteosarcoma, papillary thyroid), infection or pectus excavatum deformity. For these instances, radiologists must determine whether to use ultra-high-pitch or standard mode. When the child cannot follow directions, lie still or breath-hold, an ultra-high-pitch scan is usually suggested. A recent study has also demonstrated the utility of ultra-high-pitch low-dose CT in the setting of coronavirus disease 2019 (COVID-19) infection [28].

Fig. 4 Pulmonary blood volume technique in a 3-year-old boy born at 24 weeks of gestational age with severe bronchopulmonary dysplasia. **a** Axial CT in in lung window demonstrates hyperinflated right lung with architectural distortion. **b** Corresponding pulmonary blood volume (dense lung) tool at the same axial level demonstrates diminished perfusion to the right lung. **c, d** Coronal pulmonary blood volume (**c**) and corresponding nuclear medicine perfusion scan (**d**) (anterior view) performed the same day both show marked decreased perfusion to the right lung
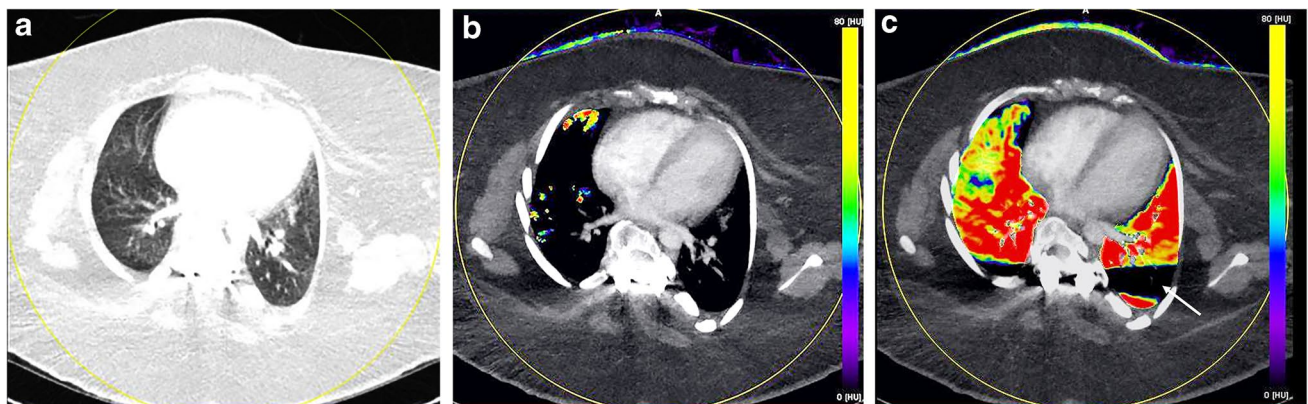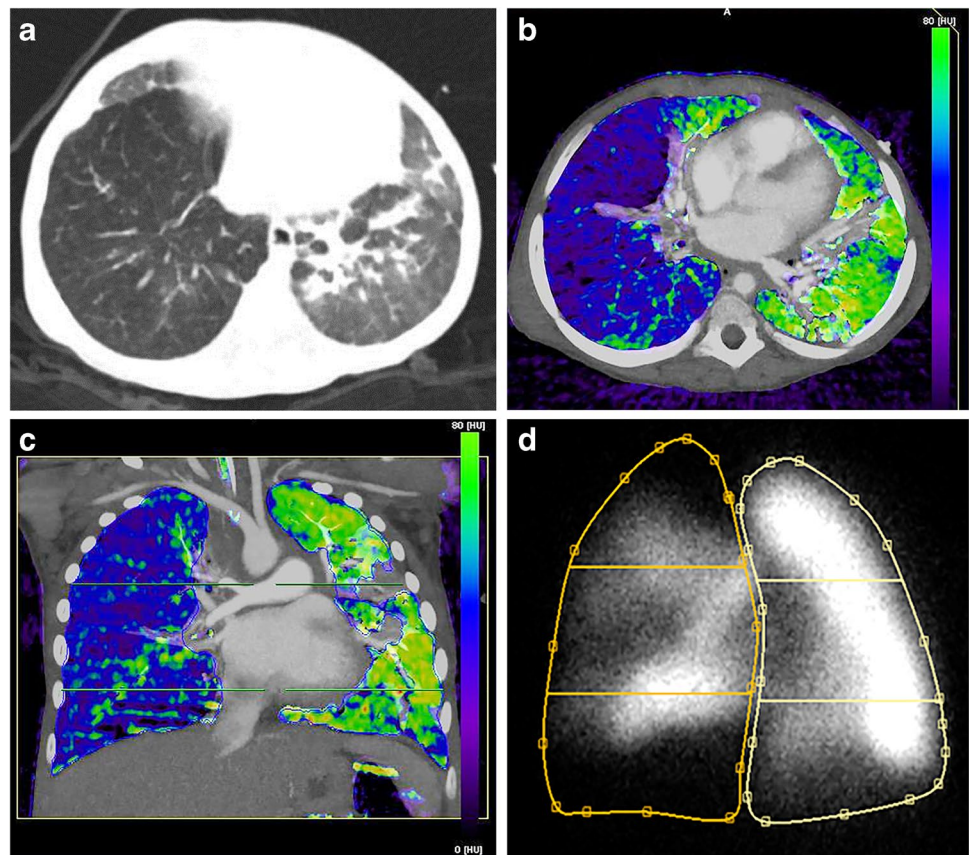

Fig. 5 CT angiogram dense lung tool in a 16-year-old girl with pulmonary embolism. This was a technically challenging study with presence of posterior spinal rods in a 125-kg patient. The study was performed on a third-generation scanner using 80 kVp/150 kVp plus tin filter. **a–c** Axial CT chest in lung window (**a**) and with lung perfusion pulmonary blood volume overlay (**b**), and axial CT with pulmonary blood volume dense lung tool (**c**). Note that despite improved perfusion map with the dense lung, artifact related to the metal persists (*arrow*). The yellow circle denotes the field-of-view limitations for the high-energy tube. No pulmonary embolism was identified

Metal artifact reduction

When metal is encountered on routine chest imaging or for the evaluation of the osseous structures of the chest, dual-energy CT can reduce metallic artifact and improve visualization of the metallic implants, the interface between the bones and the implant, and the surrounding soft tissues.

Metallic artifact results predominantly from beam-hardening and photon starvation related to metallic prosthetic material. Beam-hardening results from more

Table 2 Dual-energy post-processing options

| Exam type	Data output
CT angiography pulmonary embolism	PBV, monoenergetic+ 50 keV
CT angiography pulmonary hypertension	PBV (dense lung PBV)
Enhanced CT chest	Virtual unenhanced, iodine map
Unenhanced CT chest (metal)	Monoenergetic+ (best keV)

PBV pulmonary blood volume

low-energy photons than high-energy photons being absorbed by metallic material, resulting in a higher-energy spectrum of exiting photons. This results in a beam with decreased tissue absorption and dark streaks adjacent to the metal implants on the final image acquisition. Photon starvation occurs as the metal absorbs a large proportion of photons, causing an unfavorable signal-to-noise ratio and consequent dark streaks on the image [29]. Dual-energy CT takes advantage of the dual-energy spectra in post-processing techniques to reduce mainly beam-hardening artifacts by producing virtual monochromatic images.

Bamberg et al. [30] directly compared dual-energy monochromatic reconstruction with conventional CT imaging for subjective and objective differences in image quality and diagnostic value in subjects with metallic implants in different body parts. Both parameters were significantly improved with high-energy reconstructions and some pathology was only evident in the high-energy reconstructions [30].

High-energy virtual monoenergetic images have been shown to improve visualization of metal implants and surrounding soft tissues in various metallic hardware, without increased radiation dose. The ideal virtual monoenergetic image energy level for metal artifact reduction ranges from 108 keV to 149 keV depending on the type of metallic implant, pathological abnormality and reader preference (Fig. 6). The composition and size of the metallic prosthesis also play important roles in the success of metallic artifact reduction. Larger and denser metallic components, such as cobalt chrome joint arthroplasty, do not benefit from virtual monoenergetic imaging because the metal artifact is predominantly caused by photon starvation rather than beam-hardening. On the other hand, smaller and less dense metallic prostheses, such as titanium screws, primarily cause artifact from

Fig. 6 Metal artifact in a 17-year-old girl with chronic lung disease, arthrogryposis and posterior spinal hardware. She was imaged with dual-energy CT using 80 kVp and 140 kVp. **a–d** Sagittal CT of the chest in bone windows using the monoenergetic+ tool for reducing metal artifact at 60 keV (**a**), 80 keV (**b**), 120 keV (**c**) and 150 keV (**d**). Note how the bone surrounding the hardware is more easily resolved with progressively higher kiloelectron volts, though it is just minimally improved between 120 keV and 150 keV
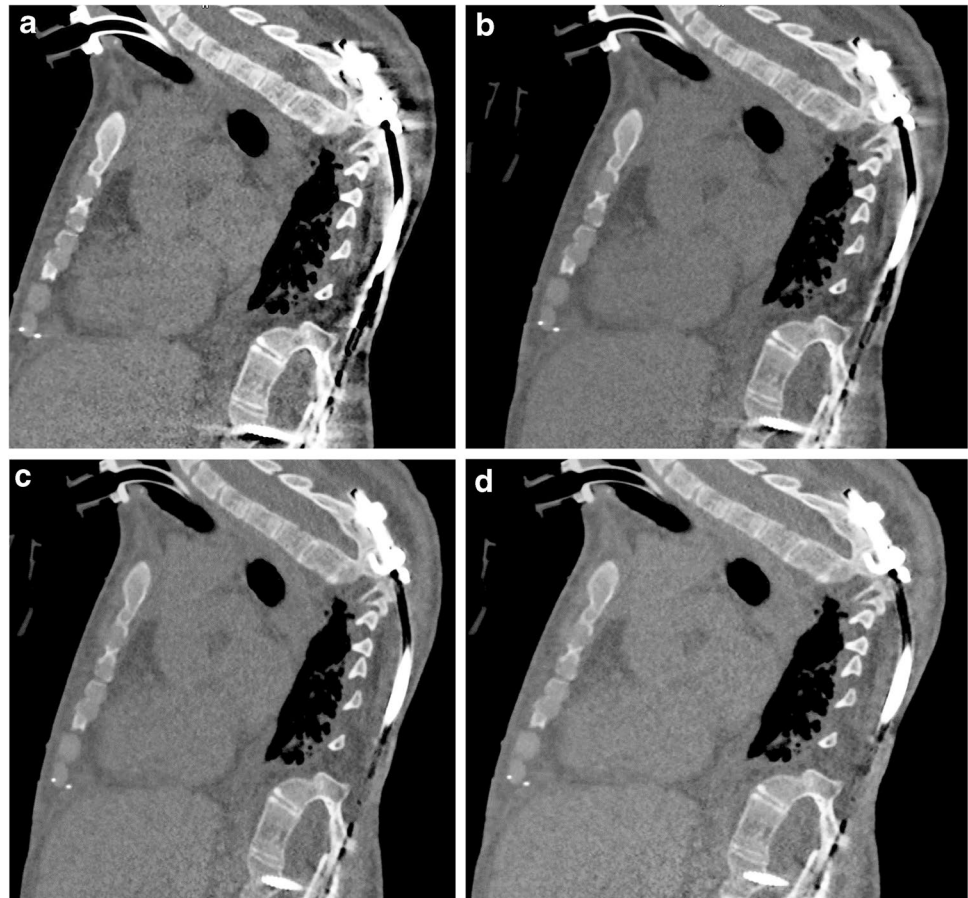
beam-hardening and thus benefit from monoenergetic imaging [31]. Kim et al. [32] described improved diagnostic performance and optimal energy levels for virtual monochromatic images (100–130 keV) compared to conventional polychromatic CT, finding that virtual monochromatic imaging reduces beam-hardening artifacts due to contrast media injection in the subclavian veins, axillary veins and superior vena cava during chest CT.

The potential downside of using the high keV for metal artifact reduction is that these keV levels are further from the k-edge of iodine, decreasing conspicuity of enhancing pathology. If intravenous (IV) contrast medium is administered, it would be beneficial to obtain a lower-keV monoenergetic image, as well, for improved contrast enhancement to complement the high-keV image.

At our institution, the CT technologist views the images at different energy levels on a case-by-case basis. Technologists then select the keV level that results in the best reduction of artifact for the body part and particular hardware encountered and sends these images to the picture archiving and communication system (PACS). The auto processing is not able to select the proper keV level due to variability of the artifacts.

Enhanced computed tomography scan

Indications for enhanced chest CT include evaluation of mediastinal lesions, primary lung mass or metastases, and soft-tissue tumors. For these indications, a study might be performed using standard CT, ultra-high-pitch CT or dual-energy CT. When a child can optimally breath-hold, a standard CT scan might be all that is necessary to have a high-quality study. Ultra-high-pitch CT is ideal for less cooperative children or to lower radiation dose. In general, dual-energy applications for these indications are not well studied in pediatrics.

Thoracic oncological applications of dual-energy imaging have only recently begun to be explored. Soft-tissue, mediastinal and lung tumors can all be evaluated using the iodine map technique. The virtual non-contrast map can be interrogated for the presence of intrinsic tumoral density or calcifications (Fig. 7). The iodine map can be assessed qualitatively and quantitatively. Regions of interest are drawn on a mass or tumor and the concentration of iodine is displayed in milligrams per milliliter (mg/mL). Studies in adults have shown that a concentration greater than 1.4 mg/mL suggests malignant tumors [33], while in children limited data

Fig. 7 Dual-energy chest CT in a 17-year-old boy with a history of pneumonia. **a–d** Axial (**a**) and sagittal (**b**) contrast-enhanced chest CT images and corresponding axial (**c**) and sagittal (**d**) virtual non-contrast images. Left-upper-lobe superior segment bronchial narrowing with post-obstructive pneumonia with a small calcification (*arrow*) is suggested on the contrast-enhanced CT (**a, b**) and confirmed on virtual non-contrast (**c, d**) images. Bronchoscopy with biopsy was performed and pathology showed endobronchial carcinoid tumor
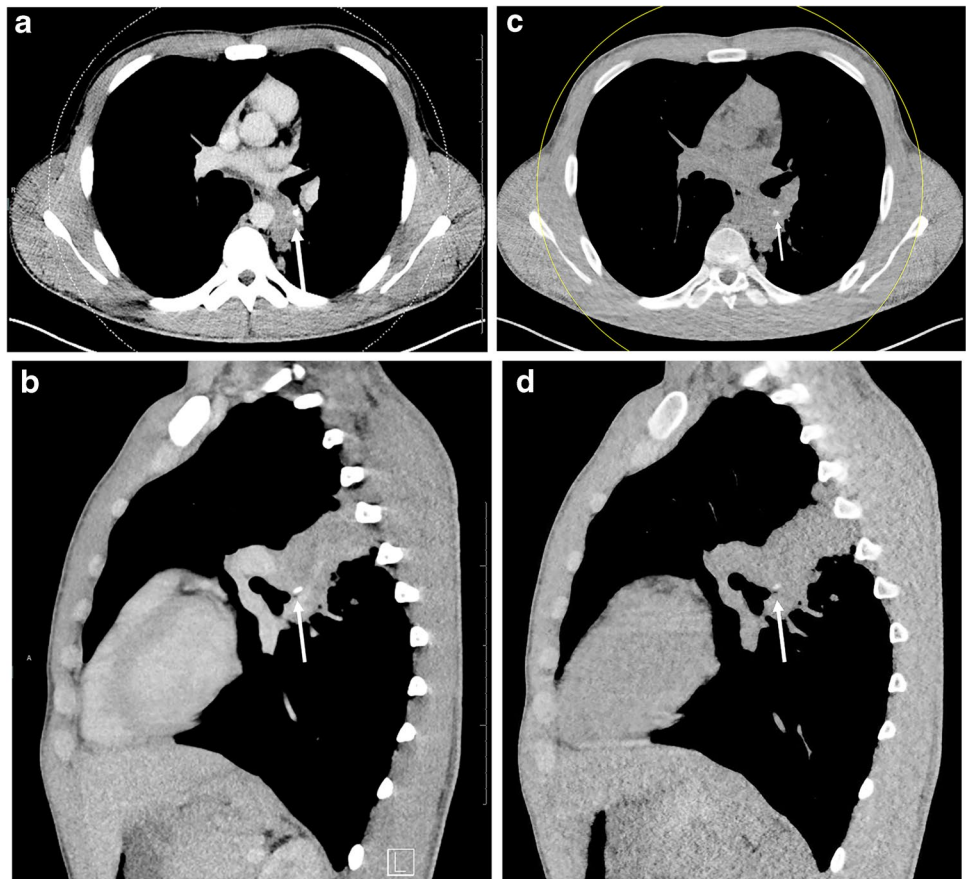
exist and a lower cutoff of 1 mg/mL has been suggested given the increased odds of malignancy when encountering a lung nodule in children [21]. Similarly, treatment response could be monitored by trending concentration of iodine over sequential scans over time, though more work is needed in this area.

Computed tomography angiography

Computed tomography has proved to be invaluable when assessing the pulmonary vascular structures including the aorta, pulmonary artery, pulmonary embolism, pulmonary hypertension and pulmonary veins [34].

When evaluating for pulmonary embolism on CT angiography, high-pitch CT angiography or dual-energy CT might be performed. When making this determination, one must take into account patient body habitus because in larger patients some tissue might fall outside the high-kVp FOV. For this reason, the child must also be centered in the CT gantry to ensure that lung tissue does not fall outside this region. If dual energy is used, several post-processing choices can be made. Pulmonary blood volume should be used to evaluate perfusion. For younger children and those with dense lungs, for example those with chronic lung disease, the dense lung tool should be employed. A low-keV monoenergetic series can prove indispensable when assessing for subtle pulmonary embolism by improving contrast enhancement. One could choose 40–70 keV to accomplish this, though we find that 50 keV obtains a balance of improved contrast because it nears the k-edge of iodine but limits the image noise seen with very low keV.

Pulmonary hypertension is a common indication for CT angiography evaluation, which is designed to examine the pulmonary artery and to assess parenchymal abnormalities. These exams are usually ultra-high-pitch scans, particularly if the child is not sedated. However, dual-energy CT can be used to assess blood flow to the parenchyma, which might decrease the need for additional nuclear medicine ventilation–perfusion scan [27]. The most important post-processing tool is the pulmonary blood volume. The dense lung pulmonary blood volume should be used when lungs are expected to be denser such as in neonates and toddlers, atelectasis, hypoventilatory changes, and in those with chronic lung disease (Figs. 4 and 5).

For vascular imaging, ECG gating is the standard of care for evaluating the aortic root (Fig. 8) [35]. Although the evaluation can be performed with prospective or retrospective gating, ECG gating with ultra-high pitch is most common. The often-overlooked vascular structures of the chest, the pulmonary veins, have been increasingly recognized as an important factor in lung perfusion and development. Although pulmonary vein evaluation can be performed without ECG gating [36], ECG gating for pulmonary vein assessment is commonly used and has demonstrated reliability when compared with conventional angiography and surgery [34]. Whether looking for anomalous pulmonary venous connections [37] or stenotic pulmonary veins [34], ultra-high-pitch dual-source imaging plays an important role in diminishing cardiac motion to aid in accurate visualization and measurement of these small structures (Fig. 9).

A CT angiography study is also performed when the indication is congenital lung lesion. While an angiographic phase is needed to look for the feeding artery and draining vein, the study does not need to be ECG-gated. One pitfall to ECG gating is that the leads need to be applied to the child, and when using the feed-and-swaddle technique in infants with suspected congenital lung lesion, the added leads can wake the child while gating might not improve imaging quality. Assessment for a suspected vascular ring can be done with or without ECG gating.

Table 3 describes dual-source techniques based on exam indications.

Scanner limitations

First, a limitation of the first-generation scanner was the effects of over-ranging, where in high-pitch scans there was additional radiation to tissues not included for imaging interpretation [16]. Because of this, some authors advocated for use of a lower pitch of about 2.0 [38]. This issue was resolved by the use of dynamic collimation on second- and third-generation scanners, allowing for ultra-high-pitch scans without over-ranging [39].

Second, while ECG gating is ideal when evaluating the heart and great vessels, it cannot be employed while utilizing dual-energy CT. This results in limitations when evaluating vascularity and perfusion of the lungs for abnormalities of the pulmonary arteries and veins. For this reason, most CT angiography studies are performed with an ECG-gated ultra-high-pitch mode instead of dual energy.

Third, as with any CT protocol, the dual-source scanners involve ionizing radiation dose to the child. The dose of each scan type, however, is equivalent to or less than the standard mode. Ultra-high-pitch imaging results in similar radiation dose as standard pitch while improving image quality [20]. Dual-energy scanning has also been shown to have favorable comparison in dose to single-energy scanning [16, 24, 40]. There have been reports of slightly higher doses in children younger than 1 year when using dual-energy mode for chest imaging with a second-generation scanner [41], though the benefits of dual energy might outweigh the small increase in radiation dose when eliminating the need for dual-phase scans or additional tests such as a nuclear medicine perfusion study [27].
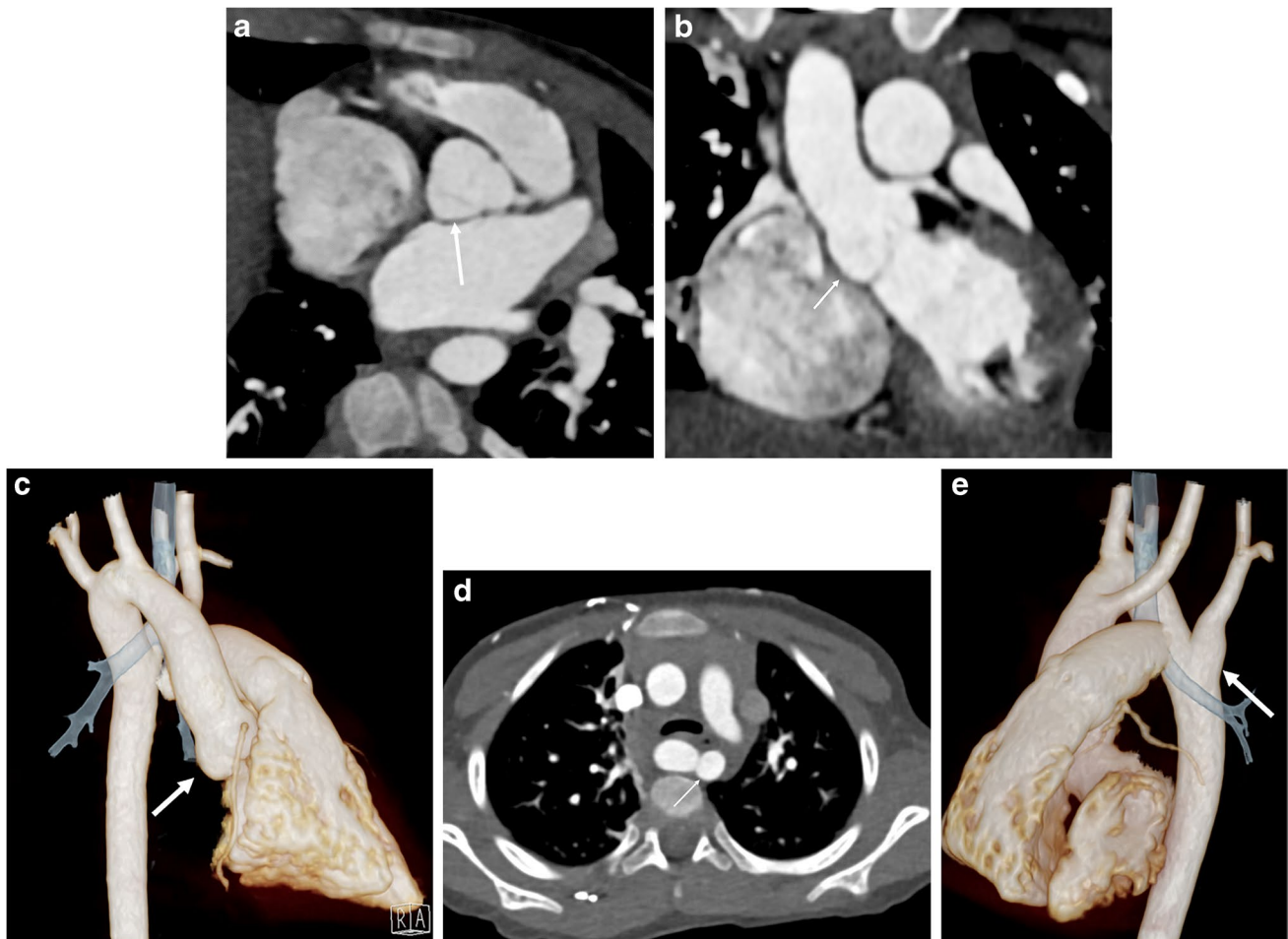
Fig. 8 CT angiography in a 4-year-old boy with suspected vascular ring and aortic root dilatation. CT angiography was performed using electrocardiography (ECG)-gated cardiac ultra-high-pitch scan technique on a second-generation scanner. **a–c** Axial oblique (**a**) and coronal oblique (**b**) to the aortic root axis images with corresponding coronal oblique three-dimensional (3-D) reformat (**c**) demonstrate a normal-size aortic root (*arrow*). **d, e** Axial CT image at the level of the aberrant subclavian artery with a diverticulum of Kommerell (*arrow*) (**d**) indicates a vascular ring; corresponding coronal oblique 3-D reformat (**e**)
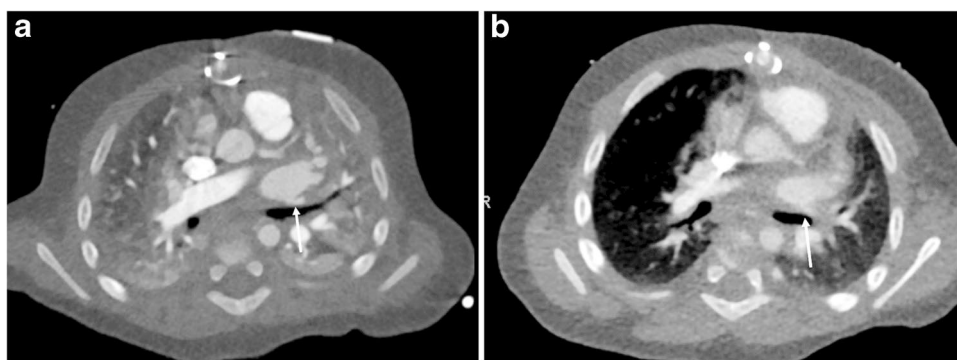

Fig. 9 CT angiography in a 5-month-old boy with pulmonary vein stenosis. **a, b** Axial CT angiogram of the chest performed with electrocardiography (ECG)-gated ultra-high-pitch flash (**a**) and dual-energy CT (**b**). Note the increased motion artifact caused by the decreased temporal resolution and lack of cardiac gating. The lingula pulmonary vein is narrowed (*arrow*) and is more easily depicted on the gated study (**a**)

Table 3 Dual-source techniques with exam indications

	Ultra-high pitch	Standard	Dual-energy
Unenhanced CT	Unable to breath-hold	Breath-hold possible	Metal
	Some lung metastasis	Some lung metastasis	
Enhanced CT	Unable to breath-hold	Breath-hold possible	Metal
	Mediastinal masses	Mediastinal masses	Tumor enhancement
	Some lung metastasis	Some lung metastasis	Lung perfusion
CT angiography			
Non-gated	Congenital lung lesion		Pulmonary hypertension
	Vascular ring		
ECG-gated	Aortic root		N/A
	Pulmonary arteries		
	Pulmonary veins		

ECG electrocardiography, *N/A* not applicable

Conclusion

Dual-source CT offers a variety of scan types to be selected based on the appropriate indication, be it for the need to decrease sedation or radiation, or to gather specific functional or diagnostic information. As long as CT remains the mainstay in diagnostic imaging, dual-source CT will continue to play a significant role in the imaging of the pediatric chest.

Declarations

Conflicts of interest None

References

1. Rapp JB, Biko DM, White AM et al (2022) Spectral imaging of the pediatric chest: past, present, and future. Pediatr Radiol. https://doi.org/10.1007/s00247-022-05404-9
2. Siegel MJ, Kaza RK, Bolus DN et al (2016) White paper of the Society of Computed Body Tomography and Magnetic Resonance on dual-energy CT, part 1: technology and terminology. J Comput Assist Tomogr 40:841–845
3. Rapp JB, Biko DM, Barrera CA et al (2020) Current and future applications of thoracic dual-energy CT in children: pearls and pitfalls of technique and interpretation. Semin Ultrasound CT MR 41:433–441
4. Sargent MA, Mceachern AM, Jamieson DH, Kahwaji R (1999) Atelectasis on pediatric chest CT: comparison of sedation techniques. Pediatr Radiol 29:509–513
5. Newman B, Krane EJ, Gawande R et al (2014) Chest CT in children: anesthesia and atelectasis. Pediatr Radiol 44:164–172
6. Tucker EW, Jain SK, Mahesh M (2017) Balancing the risks of radiation and anesthesia in pediatric patients. J Am Coll Radiol 14:1459–1461
7. Warner DO, Zaccariello MJ, Katusic SK et al (2018) Neuropsychological and behavioral outcomes after exposure of young children to procedures requiring general anesthesia: the Mayo Anesthesia Safety in Kids (MASK) study. Anesthesiology 129:89–105
8. Sun LS, Li G, Miller TLK et al (2016) Association between a single general anesthesia exposure before age 36 months and neurocognitive outcomes in later childhood. JAMA 315:2312–2320
9. Cohen MM, Cameron CB, Duncan PG (1990) Pediatric anesthesia morbidity and mortality in the perioperative period. Anesth Analg 70:160–167
10. Malviya S, Voepel-Lewis T, Eldevik OP et al (2000) Sedation and general anaesthesia in children undergoing MRI and CT: adverse events and outcomes. Br J Anaesth 84:743–748
11. Kino A, Zucker EJ, Honkanen A et al (2019) Ultrafast pediatric chest computed tomography: comparison of free-breathing vs. breath-hold imaging with and without anesthesia in young children. Pediatr Radiol 49:301–307
12. Tivnan P, Winant AJ, Johnston PR et al (2021) Thoracic CTA in infants and young children: image quality of dual-source CT (DSCT) with high-pitch spiral scan mode (turbo flash spiral mode) with or without general anesthesia with free-breathing technique. Pediatr Pulmonol 56:2660–2667
13. Schmidt B, Flohr T (2020) Principles and applications of dual source CT. Phys Med 79:36–46
14. Han BK, Rigsby CK, Hlavacek A et al (2015) Computed tomography imaging in patients with congenital heart disease part I: rationale and utility. An expert consensus document of the Society of Cardiovascular Computed Tomography (SCCT). Endorsed by the Society of [sic] Pediatric Radiology (SPR) and the North American Society of Cardiac [sic] Imaging (NASCI). J Cardiovasc Comput Tomogr 9:475–492
15. DiGeorge NW, El-ali AM, White AM et al (2020) Pediatric cardiac CT and MRI: considerations for the general radiologist. Am J Respir Crit Care Med 215:1464–1473
16. Gottumukkala RV, Kalra MK, Tabari A et al (2019) Advanced CT techniques for decreasing radiation dose, reducing sedation requirements, and optimizing image quality in children. Radiographics 39:709–726
17. Ullmann N, Secinaro A, Menchini L et al (2018) Dynamic expiratory CT: an effective non-invasive diagnostic exam for fragile children with suspected tracheo-bronchomalacia. Pediatr Pulmonol 53:73–80
18. May LA, Jadhav SP, Guillerman RP et al (2019) A novel approach using volumetric dynamic airway computed tomography to determine positive end-expiratory pressure (PEEP) settings to maintain

airway patency in ventilated infants with bronchopulmonary dysplasia. Pediatr Radiol 49:1276–1284

19. Bodelle B, Fischbach C, Booz C et al (2017) Free-breathing high-pitch 80 kVp dual-source computed tomography of the pediatric chest: image quality, presence of motion artifacts and radiation dose. Eur J Radiol 89:208–214

20. Lell MM, May M, Deak P et al (2011) High-pitch spiral computed tomography: effect on image quality and radiation dose in pediatric chest computed tomography. Investig Radiol 46:116–123

21. Siegel MJ, Bhalla S, Cullinane M (2021) Dual-energy CT material decomposition in pediatric thoracic oncology. Radiol Imaging Cancer 3:e200097

22. Leithner D, Wichmann JL, Vogl TJ et al (2017) Virtual monoenergetic imaging and iodine perfusion maps improve diagnostic accuracy of dual-energy computed tomography pulmonary angiography with suboptimal contrast attenuation. Investig Radiol 52:659–665

23. Albrecht MH, Vogl TJ, Martin SS et al (2019) Review of clinical applications for virtual monoenergetic dual-energy CT. Radiology 293:260–271

24. Siegel MJ, Ramirez-Giraldo JC (2019) Dual-energy CT in children: imaging algorithms and clinical applications. Radiology 291:286–297

25. Fuld MK, Halaweish AF, Haynes SE et al (2013) Pulmonary perfused blood volume with dual-energy CT as surrogate for pulmonary perfusion assessed with dynamic multidetector CT. Radiology 267:747–756

26. Boroto K, Remy-Jardin M, Flohr T et al (2008) Thoracic applications of dual-source CT technology. Eur J Radiol 68:375–384

27. Ramirez-Suarez KI, Barrera CA, Otero HJ et al (2021) Pilot study for comparative assessment of dual-energy CT and SPECT-CT V/Q scanning for lung perfusion evaluation in infants. Pediatr Pulmonol 57:702–710

28. Agostini A, Floridi C, Borgheresi A et al (2020) Proposal of a low-dose, long-pitch, dual-source chest CT protocol on third-generation dual-source CT using a tin filter for spectral shaping at 100 kVp for coronavirus disease 2019 (COVID-19) patients: a feasibility study. Radiol Med 125:365–373

29. Coupal TM, Mallinson PI, McLaughlin P et al (2014) Peering through the glare: using dual-energy CT to overcome the problem of metal artefacts in bone radiology. Skelet Radiol 43:567–575

30. Bamberg F, Dierks A, Nikolaou K et al (2011) Metal artifact reduction by dual energy computed tomography using monoenergetic extrapolation. Eur Radiol 21:1424–1429

31. Rajiah P, Sundaram M, Subhas N (2019) Dual-energy CT in musculoskeletal imaging: what is the role beyond gout? AJR Am J Roentgenol 213:493–505

32. Kim C, Kim D, Lee KY et al (2018) The optimal energy level of virtual monochromatic images from spectral CT for reducing beam-hardening artifacts due to contrast media in the thorax. AJR Am J Roentgenol 211:557–563

33. Lee SH, Hur J, Kim YJ et al (2013) Additional value of dual-energy CT to differentiate between benign and malignant mediastinal tumors: an initial experience. Eur J Radiol 82:2043–2049

34. Barrera CA, Saul D, Rapp JB et al (2020) Diagnostic performance of CT angiography to detect pulmonary vein stenosis in children. Int J Cardiovasc Imaging 36:141–147

35. Nagpal P, Agrawal MD, Saboo SS et al (2020) Imaging of the aortic root on high-pitch non-gated and ECG-gated CT: awareness is the key! Insights Imaging 11:51

36. Ou P, Marini D, Celermajer DS et al (2009) Non-invasive assessment of congenital pulmonary vein stenosis in children using cardiac-non-gated CT with 64-slice technology. Eur J Radiol 70:595–599

37. Well L, Weinrich JM, Meyer M et al (2021) Sensitivity of high-pitch dual-source computed tomography for the detection of anomalous pulmonary venous connection in infants. Rofo 193:551–558

38. Martine RJ, Santangelo T, Colas L et al (2017) Radiation dose levels in pediatric chest CT: experience in 499 children evaluated with dual-source single-energy CT. Pediatr Radiol 47:161–168

39. Booij R, Dijkshoorn ML, van Straten M (2017) Efficacy of a dynamic collimator for overranging dose reduction in a second- and third-generation dual source CT scanner. Eur Radiol 27:3618–3624

40. Goo HW (2013) Dual-energy lung perfusion and ventilation CT in children. Pediatr Radiol 43:298–307

41. Zhu X, Mccullough WP, Mecca P et al (2016) Dual-energy compared to single-energy CT in pediatric imaging: a phantom study for DECT clinical guidance. Pediatr Radiol 46:1671–1679